HHS Public Access

Author manuscript

J Magn Reson Imaging. Author manuscript; available in PMC 2018 April 20.

Published in final edited form as:

J Magn Reson Imaging. 2017 November ; 46(5): 1332–1340. doi:10.1002/jmri.25655.

Can Algorithmically Assessed MRI Features Predict Which Patients With a Preoperative Diagnosis of Ductal Carcinoma In Situ Are Upstaged to Invasive Breast Cancer?

Michael Harowicz, BS[1,*], **Ashirbani Saha, PhD**[1], **Lars J. Grimm, MD, MHS**[1], **P. Kelly Marcom, MD**[2], **Jeffrey R. Marks, PhD**[3], **E. Shelley Hwang, MD, MPH**[4], and **Maciej A. Mazurowski, PhD**[1,5,6]

[1]Department of Radiology, Duke University School of Medicine, Duke University, Durham, North Carolina, USA

[2]Department of Medicine, Duke University School of Medicine, Durham, North Carolina, USA

[3]Department of Surgery, Duke University School of Medicine, Durham, North Carolina, USA

[4]Department of Surgical Oncology, Duke University Medical Center, Durham, North Carolina, USA

[5]Department of Electrical and Computer Engineering, Duke University, Durham, North Carolina, USA

[6]Duke University Medical Physics Program, Durham, North Carolina, USA

Abstract

Purpose—To assess the ability of algorithmically assessed magnetic resonance imaging (MRI) features to predict the likelihood of upstaging to invasive cancer in newly diagnosed ductal carcinoma in situ (DCIS).

Materials and Methods—We identified 131 patients at our institution from 2000–2014 with a core needle biopsy-confirmed diagnosis of pure DCIS, a 1.5 or 3T preoperative bilateral breast MRI with nonfat-saturated T_1-weighted MRI sequences, no preoperative therapy before breast MRI, and no prior history of breast cancer. A fellowship-trained radiologist identified the lesion on each breast MRI using a bounding box. Twenty-nine imaging features were then computed automatically using computer algorithms based on the radiologist's annotation.

Results—The rate of upstaging of DCIS to invasive cancer in our study was 26.7% (35/131). Out of all imaging variables tested, the information measure of correlation 1, which quantifies spatial dependency in neighboring voxels of the tumor, showed the highest predictive value of upstaging with an area under the curve (AUC) = 0.719 (95% confidence interval [Cl]: 0.609–0.829). This feature was statistically significant after adjusting for tumor size ($P < 0.001$).

Conclusion—Automatically assessed MRI features may have a role in triaging which patients with a preoperative diagnosis of DCIS are at highest risk for occult invasive disease.

[*]Address reprint requests to: M.R.H., Department of Radiology, Duke University Medical Center, 2424 Erwin Rd., Ste. 3012 Durham, NC 27705. michael.harowicz@duke.edu.

Level of Evidence—4

Ductal carcinoma in situ (DCIS) is a proliferation of malignant epithelial cells that are bounded by the basement membrane of the mammary duct and thus do not metastasize to the lymph nodes.[1] However, invasive carcinoma, which invades the basement membrane, has metastatic potential and may be mammographically occult when associated with DCIS.[1] The initial diagnosis of breast cancer is routinely made using a core needle biopsy (CNB).[1] While a CNB is typically sufficient for a pathologist to make a diagnosis of DCIS, the small total volume of tumor sampled by CNB may miss adjacent invasive cancer. At the time of definitive surgery, upstaging to invasive disease occurs in 3.5–56% of cases.[2–18] A meta-analysis of DCIS upstaging rates by Brennan et al[7] concluded an average upstaging rate of 25.9%, while Lee et al[19] reviewed the literature to find an average rate of 20.9%. Because the prognostic and therapeutic implications of DCIS and invasive carcinoma differ, accurate detection of invasive cancer is clinically important. Decisions about surgery, neoadjuvant and/or adjuvant chemotherapy, radiation therapy, and hormone therapy all may be affected by the diagnosis rendered on CNB.[20–23] It is important to identify which patients with a CNB-based diagnosis of DCIS are at risk for invasive disease in order to provide optimal medical care.

Radiogenomics is an emerging field that investigates the relationship between genomic/pathology characteristics of disease and imaging phenotypes extracted by radiologists or computer algorithms.[24] National guidelines recommend the use of preoperative breast magnetic resonance imaging (MRI) for patients with either DCIS or invasive carcinoma in order to evaluate the extent of their disease.[20,22] If an imaging marker predictive of DCIS upstaging to invasive carcinoma at surgery can be identified using routine imaging, clinicians may be able to better manage patients with underestimated invasive breast cancer. Previous work using radiologist-identified features has shown that MRI has the potential to diagnose occult invasive disease in DCIS patients.[7,8,13,15,19] The purpose of this study is to expand upon this previous work by assessing the ability of semiautomatically assessed MRI features to predict DCIS upstaging to invasive carcinoma at the time of surgery.

Materials and Methods

Patient Population

Institutional Review Board approval and waiver of informed consent were secured for this study. Using our electronic database we identified all women with pathology suggesting breast cancer and a contrast-enhanced breast MRI at our institution from January 1, 2000, through March 23, 2014. We next identified patients who met the following eligibility criteria: CNB-confirmed DCIS without invasive cancer, a preoperative bilateral breast MRI with a nonfat-saturated T_1-weighted MRI sequence, no neoadjuvant therapy before breast MRI, and no prior history of breast cancer. A flowchart of patient exclusions is show in Fig. 1. The final cohort included patients with a postoperative pathologic diagnosis of either DCIS upstaged to invasive cancer ($n = 35$) or DCIS only ($n = 96$).

Imaging Data

Preoperative breast axial dynamic contrast-enhanced (DCE) MRI scans were acquired using 1.5T and 3.0T scanners in the prone position. Each study contained a precontrast nonfat-saturated T_1-weighted, a fat-saturated gradient echo T_1-weighted sequence, and a fat-saturated T_2-weighted sequence. Between two and six dynamic postcontrast T_1-weighted gradient echo series with fat suppression were obtained following intravenous administration of contrast. Specific information on the imaging protocols is in Table 1.

Clinical Data

The medical record was reviewed for the following: age at diagnosis, race/ethnicity, menopausal status, type of surgery (breast conservation surgery, mastectomy, no surgery), neoadjuvant and/or adjuvant therapy (radiation, chemotherapy, hormone therapy). The data from the histopathology reports included the following: receptor status (estrogen receptor [ER], progesterone receptor [PR], human epidermal growth factor 2 [HER2]), Ki-67, TNM staging,[25] tumor grade (based on the Nottingham grading system), and histologic type. An Allred score from immunohistochemical (IHC) stain of greater than or equal to 3 was considered positive for ER and PR status.[26] HER2 status was reported by using IHC according to the College of American Pathologist/American Society of Clinical Oncology (CAP/ASCO) guidelines.[27] Scores of 0 and 1 + were considered negative. A score of 3 + was considered positive. If the IHC score was 2+, then receptor status was based on the fluorescence in situ hybridization (FISH) result. A HER2:- CEP17 ratio <1.8 was considered negative for HER2, ratio of 1.8-2.2 was equivocal, and ratio >2.2 was positive. Stereotactic biopsies were done using a 9G needle and a vacuum-assisted method. Patients had a range of one to six core needle biopsies before surgery. The process of inspection of pathological samples involves microscopic examination of hematoxylin and eosin (H&E)-stained slides that represent all blocks from biopsy and surgical procedures. An interpretation of the pathology present was noted for each slide.

Image Annotation

Each case was annotated by one fellowship-trained breast-imaging radiologist with 1 year of experience (L.J.G.). For each case the reader identified one lesion (mass/nonmass enhancement) by drawing a 2D box around the lesion using an in-house graphical user interface (GUI). The reader then selected the range of slices that encompassed the totality of the lesion. The T_1-weighted precontrast fat-saturated sequence, T_1-weighted postcontrast fat-saturated sequence, and subtraction between these two sequences were provided to the reader through the GUI. The following information was provided to the radiologist to help identify the biopsied lesion: breast CNB location of the DCIS collected from the medical record and access to the MRI exam in our institutions picture archiving and communication system (PACS).

Computer-Based Image Segmentation and Feature Extraction

Based on the radiologists annotation, the lesion was segmented using a fuzzy c-means (FCM) clustering algorithm[28] on the subtracted series of images, which are computed using the precontrast and first postcontrast sequence. The imaging features were then computed

using the segmented tumor. It has been established earlier in the work of Esserman et al[29] that imaging features from MRI indicative of tumor size, distribution, and enhancement patterns for DCIS patients correlate with tumor biology. Hence, we extracted a set of imaging features pertaining to tumor morphology, textural properties, and enhancement in MRI for our investigation. A total of 29 imaging features were extracted from each case. The details of these features are as follows.

TUMOR MORPHOLOGIC FEATURES REPRESENTATIVE OF DIFFERENT ASPECTS OF TUMOR, SIZE, COMPACTNESS, APPEARANCE, AND DENSITY (9 FEATURES)—Algorithmically extracted major axis (indicative of tumor size), median value of lesion elongation (ratio of major axis to minor axis) over all slices, median solidity, median Euler number (measures of the compactness of the lesion voxels) over all slices, bounding ellipsoid volume ratio (BEVR),[30] bounding ellipsoid diameter ratio 1 (BEDR1), bounding ellipsoid diameter ratio 2 (BEDR2), margin fluctuation (MF),[31,32] and angular standard deviation (ASD)[33] are computed to assess different shape and size-based properties of the lesions. These features are representative of different aspects of tumor, size, compactness, appearance, and density.

TUMOR TEXTURAL FEATURES QUANTIFYING TEXTURAL FEATURES OF THE LESION (16 FEATURES)—From the segmented tumor, the smallest convex polygon encompassing the 3D lesion is determined. Then a gray-level co-occurrence matrix (GLCM) is populated using the first postcontrast sequence, and the smallest convex polygon using all the voxels from the segmented lesion. Sixteen textural features[34] are then computed using this GLCM. These features include autocorrelation, contrast, correlation, cluster prominence, cluster shade, dissimilarity, energy, entropy, homogeneity, maximum probability, sum average, sum variance, sum entropy, sum of squares variance, information measure of correlation 1 (IMC1), and information measure of correlation2. These textural features capture various aspects of tumor distribution inside the smallest convex polygon encompassing the 3D lesion after the segmentation.

MRI ENHANCEMENT FEATURES QUANTIFYING BREAST ENHANCEMENT DYNAMICS (4 FEATURES)—A total of three of these features are based on the background parenchyma enhancement quantifying the proportion of background parenchyma enhancing more than 10%, variance of the proportion of background parenchyma enhancing more than 10-100% in steps of 10%, and index of dispersion of the proportion of background parenchyma enhancing more than 10-100%. The fourth feature (FI) combines both lesion and parenchyma enhancement dynamics as mentioned in Mazurowski et al.[35] These enhancement dynamics features capture enhancement patterns of breast parenchyma, as well as tumor and parenchyma together.

Statistical Analysis

To test whether each of the examined imaging variables was associated with upstaging, we constructed a univariate logistic regression model for each of the variables, which gave us the unadjusted *P*- values. We then controlled for tumor size to ensure that the predictive value of the computer-extracted features is not simply reduced to this simple measurement.

To do so, we constructed a two- variable logistic regression model for each imaging variable where the covariates were the imaging features and the tumor size, which gave us the adjusted *P*-values. The significance level for our study was 0.0017 (0.05/31), as we considered 31 features. To quantify how well each feature predicted upstaging, we calculated area under the receiver operating characteristic (ROC) curve (AUC) and associated confidence intervals (CIs).

As an additional exploratory analysis, we evaluated the potential of a multivariate model for predicting upstaging, we first selected features using the entire dataset with a backward stepwise feature selection algorithm. Then we constructed a multivariate logistic regression model and evaluated it in a leave-one-out cross-validation setting. We noted a potential bias to this approach due to the features being selected outside of the cross-validation loop. Therefore, the results correspond to an upper bound of an achievable performance given our sample size, which is appropriate due to the preliminary character of this analysis. To estimate the multivariate classifier performance, similarly as for the univariate analysis, we calculated the AUC with its CIs.

Results

The upstaging rate in the overall cohort was 26.7%. The clinicopathologic characteristics associated with DCIS upstaging and pure DCIS are shown in Table 2. The association strength in terms of AUC performance for each of the analyzed imaging variables is shown in Fig. 2 and Table 3. The features contrast, correlation 1, dissimilarity, energy, entropy, homogeneity, max probability, sum entropy, and IMC1 all had a *P*-value of less than 0.05. After correcting for multiple hypothesis testing, the feature IMC1 still had a statistically significant *P*-value of 0.0008 after controlling for the tumor size in terms of the algorithmically computed major axis length of the tumor. Figure 3 shows two representative cases of DCIS and DCIS upstaged to invasive car cinoma with the corresponding values of the feature IMC1. Higher absolute values of IMC1, which is indicative of higher dependence between all center voxels and their corresponding neighboring voxels inside the convex polygon bounding the tumor, denote a higher possibility of upstaging.

The exploratory analysis multivariate model showed no improvement as compared to the most predictive individual feature. The performance of the multivariate model was AUC = 0.717 (95% CI: 0.814-0.620). We concluded that, given the limited sample size, there was no considerable improvement to be gained by combining the features. The features selected to the multivariate model were FI ($T_1 1 = 0.02$, $T_1 2 = 0.5$), bounding ellipsoid volume ratio, autocorrelation, contrast, cluster prominence, cluster shade, dissimilarity, energy, homogeneity, maximum probability, sum variance, and IMC1.

A total of 16 cases were excluded from the study because a lesion was not visible on MRI. None of these cases were upstaged to invasive carcinoma. Most of these patients had lesions that were small or did not have a lesion present at surgery with the following distribution: 7 out of the 16 patients had lesions that were measured at 1.0 cm or less at the time of surgery, four patients did not have DCIS present at surgery, three had lesions greater than 1.0 cm, and two had unavailable tumor size. The majority of these 16 patients had high-grade DCIS with

the breakdown of grade as follows: zero were grade 1, four were grade 2, 11 were grade 3, and one had unavailable pathologic grade. Also, most these patients were ER- and PR-positive as follows: 12 ER- and PR-positive, three ER- and PR-negative, and one with unavailable hormone receptor data. The ER and PR breakdown of these 16 is similar to that of the rest of the DCIS-only patients with 75% being positive. More of these patients had high-grade disease (68.8%) as compared to the 51% in the rest of the DCIS-only cases.

Discussion

Upstaging of DCIS to invasive carcinoma has implications for treatment planning. In this dataset, the rate of upstaging from DCIS to DCIS with an invasive component was within the ranges previously identified[2–18] and similar to the average rate of upstaging found in Brennan et al[7] and Lee et al.[19] Our study shows that semiautomatically assessed MRI features may have a role in predicting patients with a preoperative diagnosis of DCIS who are at increased risk for having an invasive component to their disease.

Several of the digitally extracted features had notable predictive value, but the feature IMC1 is the most promising out of all of the features. IMC1 computes the relationship between a voxel and its neighboring voxels from an information-theoretic point of view. The proximity of IMC1 to zero indicates that a voxel can be predicted with less certainty from the neighboring voxels. In our results, higher absolute values (hence, farther from zero) of IMC1 are indicative of upstaging. Therefore, for cases upstaged to invasive cancer a voxel can be predicted with higher certainty than that of DCIS. DCIS cases exhibit a sponge-like appearance, which increases the uncertainty in the prediction of neighboring voxels and therefore lower absolute values of IMCl are obtained. However, for upstaging, the tumor has a more solid and smooth appearance, which increases the absolute value of IMCl.

Previous studies have examined several variables that may be predictive of DCIS with an invasive component including the following: clinical characteristics,[2,10,16,17] histopathologic characteristics,[3,4,6–12,16] and imaging characteristics [2,3,5,7,9,12,13,18] The imaging characteristics previously studied were the presence of a mass, enhancement kinetics, enhancement washout, lesion size on imaging, signal intensity on MRI, heterogeneous or rim enhancement pattern on MRI, and apparent diffusion coefficient (ADC). However, Lee et al[19] discussed that there have been inconclusive findings for several of these imaging features. Our study expanded on these previously investigated imaging variables by examining automatically assessed imaging features on MRI and showed that those features might be useful in prediction of upstaging of DCIS.

There are major advantages to the use of automatically assessed features as opposed to subjective measures such as radiologist-perception based features. The algorithmic assessment of features allows for a more comprehensive and standardized assessment of tumor characteristics. The interobserver variability between radiologists is also mitigated by this approach, as opposed to perception-based measures. The radiologist's role in the use of these automatic features is to annotate a bounding box around the lesion of interest on the MRI. Although interobserver variability is still present in the algorithmic approach, the variability is alleviated by automatic segmentation of the tumor and the variability has been

shown to not translate into considerable variability for the assessment of enhancement dynamics.[36] The use of these automatically assessed imaging features would minimally affect the workflow of the radiologist, while providing valuable information to the patients treatment team.

Our study is limited by its retrospective singleinstitution design and small sample size. Despite these limitations, we found that our automatically extracted MRI feature IMC1 was predictive of DCIS with an invasive component. Further validation and extension of these results in larger datasets is needed, which might reveal other prognostic variables or multivariate models superior to the one presented in this study. However, our analysis supports that automated image analysis of digital MRI images can predict the presence of concurrent invasive cancer with a high predictive value. Finally, the data used in this study spans 16 years, during which some changes were made to the imaging equipment. Some improvement in prognostic value of the imaging features could be seen in a more homogeneous cohort.

Please note that 16 patients were excluded from our analysis since they were not visible on MRI.

None of these cases were upstaged to invasive carcinoma, suggesting that visibility of the lesion on MRI is strongly associated with upstaging, which is consistent with the results shown in Hwang et al.[37] The results presented in this study are applicable only to tumors that are visible on MRI.

Additional studies will be required to determine whether one or a group of automatically extracted radiologic features can accurately discriminate pure DCIS from DCIS with invasive cancer, and whether the performance of these features exceeds that of radiologist interpretation alone. Further, the value of this clinical information must be considered in light of the costs incurred by this additional testing, as well as which patients with DCIS would be most likely to benefit. This is especially a concern, as several studies have shown increased mastectomy rates associated with use of preoperative breast MRI.[38–40] The future role for such radiogenomic approaches could lie in their ability to mitigate the interobserver variability inherent in single radiologist interpretation, and the potential for their use as a component of integrated diagnostic tools that can be refined to predict tumor biology.

Acknowledgments

Contract grant sponsor: National Institutes of Health; contract grant number: 1R01EB021360 (to M.M.); 5R01CA185I38-02 (to E.S.H.); Contract grant sponsor: Department of Defense Award; contract grant number: BC132057 (to E.S.H.); Contract grant sponsor: North Carolina Biotechnology Center BIG grant (to M.M.).

References

1. Virnig BA, Tuttle TM, Shamliyan T, Kane RL. Ductal carcinoma in situ of the breast: a systematic review of incidence, treatment, and outcomes. J Natl Cancer Inst. 2010; 102:170–178. [PubMed: 20071685]
2. Goyal A, Douglas-Jones A, Monypenny I, Sweetland H, Stevens G, Mansel RE. Is there a role of sentinel lymph node biopsy in ductal carcinoma in situ?: Analysis of 587 cases. Breast Cancer Res Treat. 2006; 98:311–314. [PubMed: 16552627]

3. Dillon MF, McDermott EW, Quinn CM, O'Doherty A, O'Higgins N, Hill AD. Predictors of invasive disease in breast cancer when core biopsy demonstrates DCIS only. J Surg Oncol. 2006; 93:559–563. [PubMed: 16705731]
4. Rutstein LA, Johnson RR, Poller WR, et al. Predictors of residual invasive disease after core needle biopsy diagnosis of ductal carcinoma in situ. Breast J. 2007; 13:251–257. [PubMed: 17461899]
5. Lee JW, Han W, Ko E, et al. Sonographic lesion size of ductal carcinoma in situ as a preoperative predictor for the presence of an invasive focus. J Surg Oncol. 2008; 98:15–20. [PubMed: 18459155]
6. Go EM, Chan SK, Vong JS, et al. Predictors of invasion in needle core biopsies of the breast with ductal carcinoma in situ. Mod Pathol. 2010; 23:737–742. [PubMed: 20081814]
7. Brennan ME, Turner RM, Ciatto S, et al. Ductal carcinoma in situ at core-needle biopsy: meta-analysis of underestimation and predictors of invasive breast cancer. Radiology. 2011; 260:119–128. [PubMed: 21493791]
8. Huang YT, Cheung YC, Lo YF, Ueng SH, Kuo WL, Chen SC. MRI findings of cancers preoperatively diagnosed as pure DCIS at core needle biopsy. Acta Radiol. 2011; 52:1064–1068. [PubMed: 21969708]
9. Han JS, Molberg KH, Sarode V. Predictors of invasion and axillary lymph node metastasis in patients with a core biopsy diagnosis of ductal carcinoma in situ: an analysis of 255 cases. Breast J. 2011; 17:223–229. [PubMed: 21545433]
10. Kim J, Han W, Lee JW, et al. Factors associated with upstaging from ductal carcinoma in situ following core needle biopsy to invasive cancer in subsequent surgical excision. Breast. 2012; 21:641–645. [PubMed: 22749854]
11. Hollingsworth AB, Stough RG. Multicentric and contralateral invasive tumors identified with pre-op MRI in patients newly diagnosed with ductal carcinoma in situ of the breast. Breast J. 2012; 18:420–427. [PubMed: 22804792]
12. Trentin C, Dominelli V, Maisonneuve P, et al. Predictors of invasive breast cancer and lymph node involvement in ductal carcinoma in situ initially diagnosed by vacuum-assisted breast biopsy: experience of 733 cases. Breast. 2012; 21:635–640. [PubMed: 22795363]
13. Goto M, Yuen S, Akazawa K, et al. The role of breast MR imaging in pre-operative determination of invasive disease for ductal carcinoma in situ diagnosed by needle biopsy. Eur Radiol. 2012; 22:1255–1264. [PubMed: 22205445]
14. Mori N, Ota H, Mugikura S, et al. Detection of invasive components in cases of breast ductal carcinoma in situ on biopsy by using apparent diffusion coefficient MR parameters. Eur Radiol. 2013; 23:2705–2712. [PubMed: 23732688]
15. Wisner DJ, Hwang ES, Chang CB, et al. Features of occult invasion in biopsy-proven DCIS at breast MRI. Breast J. 2013; 19:650–658. [PubMed: 24165314]
16. Guillot E, Vaysse C, Goetgeluck J, et al. Extensive pure ductal carcinoma in situ of the breast: identification of predictors of associated infiltrating carcinoma and lymph node metastasis before immediate reconstructive surgery. Breast. 2014; 23:97–103. [PubMed: 24388733]
17. Park AY, Gweon HM, Son EJ, Yoo M, Kim JA, Youk HJ. Ductal carcinoma in situ diagnosed at US-guided 14-gauge core-needle biopsy for breast mass: preoperative predictors of invasive breast cancer. Eur J Radiol. 2014; 83:654–659. [PubMed: 24534119]
18. Nadrljanski M, Maksimovic R, Plesinac-Karapandzic V, Nikitovic M, Markovic-Vasiljkovic B, Milosevic Z. Positive enhancement integral values in dynamic contrast enhanced magnetic resonance imaging of breast carcinoma: ductal carcinoma in situ vs. invasive ductal carcinoma. Eur J Radiol. 2014; 83:1363–1367. [PubMed: 24894697]
19. Lee CW, Wu HK, Lai HW, et al. Preoperative clinicopathologic factors and breast magnetic resonance imaging features can predict ductal carcinoma in situ with invasive components. Eur J Radiol. 2016; 85:780–789. [PubMed: 26971424]
20. Coates AS, Winer EP, Goldhirsch A, et al. Tailoring therapies— improving the management of early breast cancer: St Gallen International Expert Consensus on the Primary Therapy of Early Breast Cancer 2015. Ann Oncol. 2015; 26:1533–1546. [PubMed: 25939896]
21. Mitchell KB, Kuerer H. Ductal carcinoma in situ: treatment update and current trends. Curr Oncol Rep. 2015; 17:48. [PubMed: 26373411]

22. Kaufman SA, Harris EE, Bailey L, et al. ACR appropriateness criteria(R) ductal carcinoma in situ. Oncology. 2015; 29:441–460.
23. Bellon JR, Harris EE, Arthur DW, et al. American College of, R. ACR Appropriateness Criteria(R) conservative surgery and radiation—stage I and II breast carcinoma: expert panel on radiation oncology: breast. Breast J. 2011; 17:448–55. [PubMed: 21790842]
24. Mazurowski MA. Radiogenomics: what it is and why it is important. J Am Coll Radiol. 2015; 12:862–866. [PubMed: 26250979]
25. Edge SB, Compton CC. The American Joint Committee on Cancer: the 7th edition of the AJCC cancer staging manual and the future of TNM. Ann Surg Oncol. 2010; 17:1471–1474. [PubMed: 20180029]
26. Calhoun BC, Collins LC. Predictive markers in breast cancer, An update on ER and HER2 testing and reporting. Semin Diagn Pathol. 2015; 32:362–369. [PubMed: 25770732]
27. Wolff AC, Hammond ME, Schwartz JN, et al. American Society of Clinical Oncology/College of American Pathologists guideline recommendations for human epidermal growth factor receptor 2 testing in breast cancer. J Clin Oncol. 2007; 25:118–145. [PubMed: 17159189]
28. Bezdek, JC. Pattern recognition with fuzzy objective function algorithms. Amsterdam: Kluwer Academic Publishers; 1981.
29. Esserman LJ, Kumar AS, Herrera AF, et al. Magnetic resonance imaging captures the biology of ductal carcinoma in situ. J Clin Oncol. 2006; 24:4603–4610. [PubMed: 17008702]
30. Mazurowski MA, Czamek NM, Collins LM, Peters KB, Clark K. Predicting outcomes in glioblastoma patients using computerized analysis of tumor shape: preliminary data. SPIE Proc. 2016; 9785 97852T-97852T-6.
31. Giger ML, Vybomy CJ, Schmidt RA. Computerized characterization of mammographic masses: analysis of spiculation. Cancer Lett. 1994; 77:201–211. [PubMed: 8168067]
32. Pohlman S, Powell KA, Obuchowski NA, Chilcote WA, Grundfest-Broniatowski S. Quantitative classification of breast tumors in digitized mammograms. Med Phys. 1996; 23:1337–1345. [PubMed: 8873030]
33. Georgiou H, Mavroforakis M, Dimitropoulos N, Cavouras D, Theodoridis S. Multi-scaled morphological features for the characterization of mammographic masses using statistical classification schemes. Artif Intell Med. 2007; 41:39–55. [PubMed: 17714924]
34. Haralick RM, Shanmugam K, Dinstein IH. Textural features for image classification. IEEE Trans Syst Man Cybernet. 1973; 3:610–621.
35. Mazurowski MA, Zhang J, Grimm LJ, Yoon SC, Silber JI. Radiogeomic analysis of breast cancer: Luminal B molecular subtype is associated with enhancement dynamics at MR imaging. Radiology. 2014; 273:365–372. [PubMed: 25028781]
36. Saha A, Grimm LJ, Harowicz M, et al. Interobserver variability in identification of breast tumors in MRI and its implications for prognostic biomarkers and radiogenomics. Med Phys. 2016; 43:4558. [PubMed: 27487872]
37. Hwang ES, Kinkel K, Esserman LJ, Lu Y, Weidner N, Hylton N. Magnetic resonance imaging in patients diagnosed with ductal carcinoma-in-situ: value in the diagnosis of residual disease occult invasion, and multicentricity. Ann Surg Oncol. 2003; 10:381–388. [PubMed: 12734086]
38. Chandwani S, George PA, Azu M, et al. Role of preoperative magnetic resonance imaging in the surgical management of early-stage breast cancer. Ann Surg Oncol. 2014; 21:3473–3480. [PubMed: 24912611]
39. Itakura K, Lessing J, Sakata T, et al. The impact of preoperative magnetic resonance imaging on surgical treatment and outcomes for ductal carcinoma in situ. Clin Breast Cancer. 2011; 11:33–38. [PubMed: 21421520]
40. Fancellu A, Soro D, Castiglia P, et al. Usefulness of magnetic resonance in patients with invasive cancer eligible for breast conservation: A comparative study. Clin Breast Cancer. 2014; 14:114–121. [PubMed: 24321101]

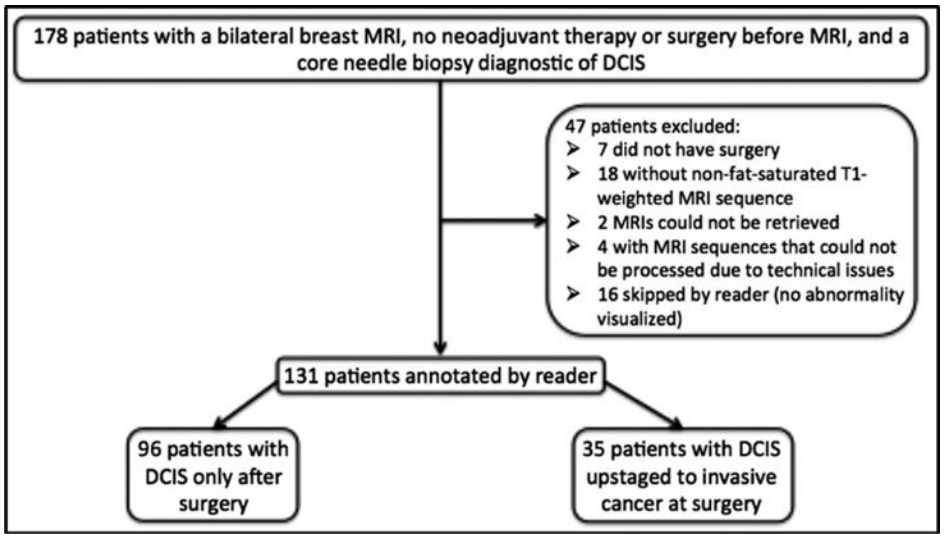

FIGURE 1.
Flow chart of patient exclusion criteria.

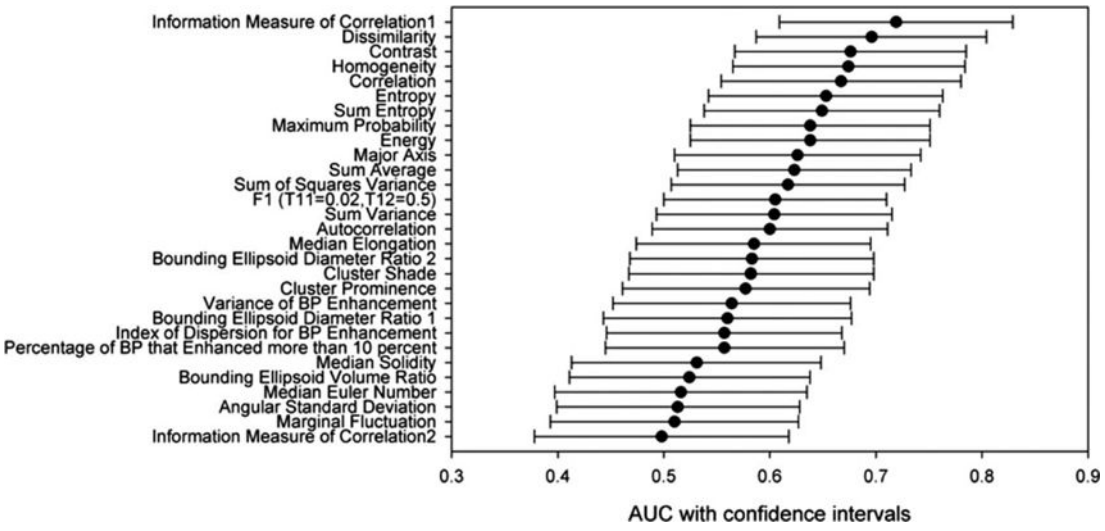

FIGURE 2.

AUC with confidence intervals for the 29 features obtained after univariate logistic regression fitting.

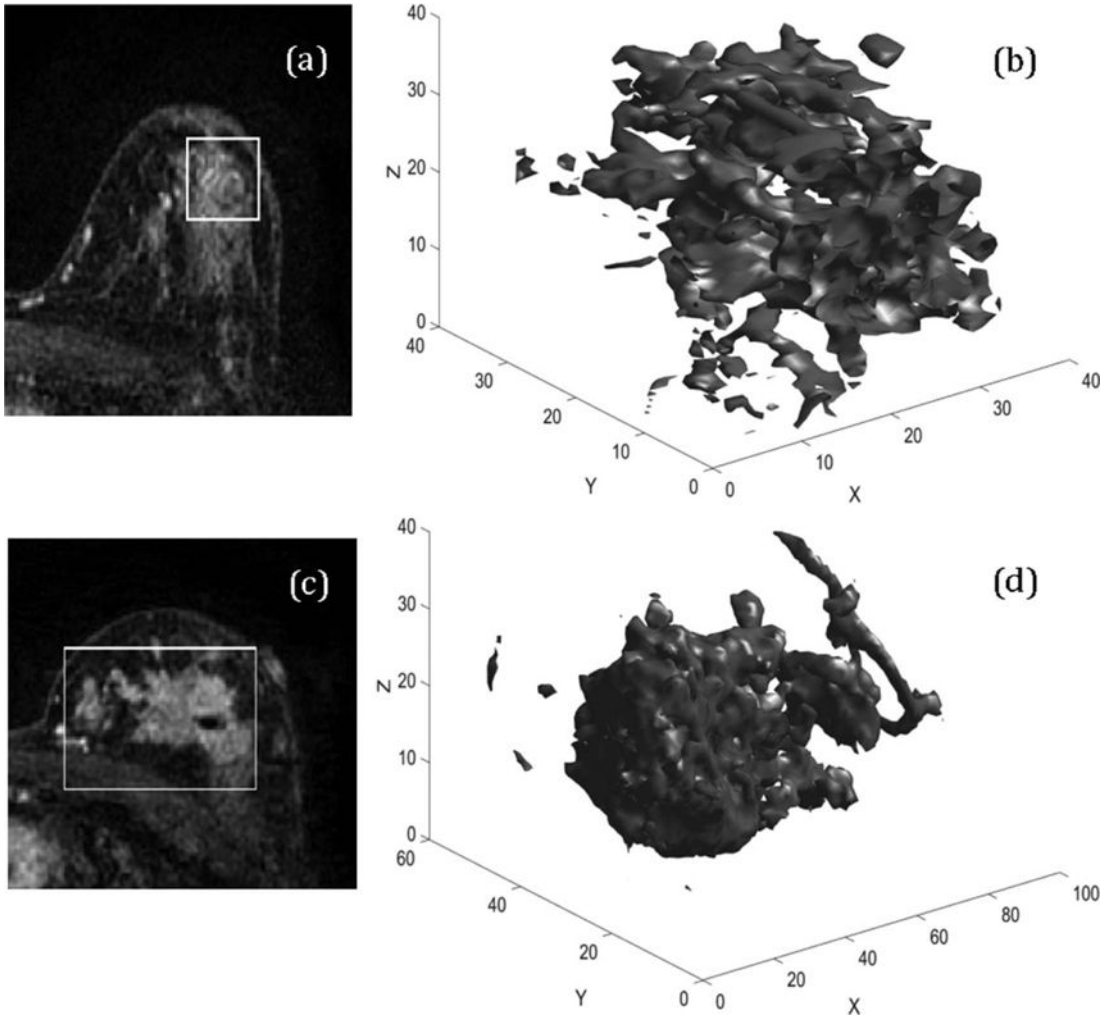

FIGURE 3.

3D representation of DCIS and DCIS upstaged to invasive carcinoma. a,c: Two central slices from the first postcontrast sequence of DCIS and DCIS upstaged to Invasive carcinoma using the radiologists annotation. b,d: The 3D renderings of the automatically segmented tumor. The values of the feature information measure of correlation1 are 0.1573 and 0.3919, respectively.

TABLE 1

MRI Protocols for Dynamic Contrast-Enhanced Sequences

Scanner Model	Field strength (T)	FOV (cm)	Matrix Size	TE (msec)	TR (msec)
MAGNETOM Avanto	1.5	36	448 × 448	1.3	4.0
MAGNETOM Trio	3.0	36	448 × 448	1.4	4.1
Signa HDx/HDxt	1.5	38	350×350	2.4	5.3
Signa HDx	3.0	34	350×350	2.4	5.7

TABLE 2

Clinicopathologic Characteristics of Ductal Carcinoma In Situ With and Without Invasive Carcinoma

variable	Subvariable	DCIS upstaged to invasive carcinoma at surgery	DCIS only	*P* value
n		35	96	
Age, mean (range)		50.5 (32.5-80.7)	53.4 (31.0-75.2)	0.1935
Menopausal status (%)	Premenopausal	16 (45.7%)	45 (46.9%)	1
	Postmenopausal	18 (51.4%)	50 (52.1%)	
	Not reported	1 (2.9%)	1 (1.0%)	
Race/Ethnicity (%)	White	27 (77.1%)	73 (76.1%)	0.7254
	Black	4 (11.4%)	18 (18.8%)	
	Asian	0	2 (2.1%)	
	Native American	0	1 (1.0%)	
	Hispanic	1 (2.9%)	1 (1.0%)	
	Multiracial	1 (2.9%)	0	
	Not reported	2 (5.7%)	1 (1.0%)	
Nottingham grade (%)	Low	1 (2.9%)	NA	NA
	Intermediate	16 (45.7%)	NA	
	High	12 (34.3%)	NA	
	Not reported	6 (17.1%)	NA	
Nuclear grade (%)	Low	0	6 (6.3%)	0.1124
	Intermediate	11 (31.4%)	40 (41.7%)	
	High	24 (68.6%)	49 (51.0%)	
	Not reported	0	1 (1.0%)	
T stage (%)	1	29 (82.9%)	NA	NA
	2	4 (11.3%)	NA	
	3	1 (2.9%)	NA	
	4	0	NA	
	Not reported	1 (2.9%)	NA	
N stage (%)	0	26 (74.3%)	NA	NA
	1	5 (14.2%)	NA	
	2	0	NA	
	3	1 (2.9%)	NA	
	Not reported	3 (8.6%)	NA	
M stage (%)	0	33 (94.2%)	NA	NA
	1	1 (2.9%)	NA	
	Not reported	1 (2.9%)	NA	
ER status (%)	Positive	19 (54.2%)	80 (83.3%)	0.0002346
	Negative	15 (42.9%)	11 (11.5%)	
	Not reported	1 (2.9%)	5 (5.2%)	
PR status (%)	Positive	16 (45.7%)	70 (72.9%)	0.00279

variable	**Subvariable**	**DCIS upstaged to invasive carcinoma at surgery**	**DCIS only**	***P* value**
	Negative	18 (51.4%)	21 (21.9%)	
Variable	Subvariable	DCIS upstaged to invasive carcinoma at surgery	DCIS only	*P* value
	Not reported	1 (2.9%)	5 (5.2%)	
HER2 status (%)	Positive	9 (25.7%)	NA	NA
	Negative	25 (71.4%)	NA	
	Not reponed	1 (2.9%)	NA	
Ki-67 mean (range)		43.6 (5-90)	NA	NA

The following variables were tested using the Pearson's chi-squared test with Yates' continuity correction: menopausal status, race/ethnicity, ER, and PR. Race/ethnicity testing was binarized to white and nonwhite. Age was tested using the Welch Two Sample t-test. Nuclear grade was tested using Pearsons's chi-squared test with simulated P-value.

TABLE 3

Univariate Logistic Regression of MRI Features for Prediction of DCIS With an Invasive Component

MRI feature	AUC	AUC confidence interval	*P*-value	*P*-value (adjusted)
Major axis	0.626	(0.510-0.742)	0.0387	NA
BEVR	0.524	(0.411-0.638)	0.906	0.135
BEDR1	0.560	(0.443-0.677)	0.256	0.452
BEDR2	0.583	(0.468-0.698)	0.149	0.221
MF	0.510	(0.393-0.627)	0.954	0.210
ASD	0.513	(0.399-0.628)	0.879	0.559
Median solidity	0.531	(0.413-0.648)	0.818	0.0752
Median elongation	0.585	(0.474-0.695)	0.307	0.530
Median Euler no	0.516	(0.397-0.635)	0.664	0.130
autocorrelation	0.600	(0.489-0.711)	0.385	0.780
Contrast	0.676	(0.567-0.785)	0.0231	0.157
Correlation 1	0.667	(0.554-0.780)	0.00441	0.0106
Cluster prominence	0.577	(0.461-0.694)	0.438	0.656
Cluster shade	0.582	(0.467-0.698)	0.284	0.875
Dissimilarity	0.696	(0.587-0.804)	0.00872	0.0587
Energy	0.638	(0.525-0.751)	0.0258	0.157
Entropy	0.653	(0.542-0.763)	0.017	0.112
Homogeneity l	0.674	(0.565-0.784)	0.0109	0.0718
Max probability	0.638	(0.525-0.751)	0.0361	0.201
Sum of squares variance	0.617	(0.507-0.727)	0.236	0.963
Sum average	0.623	(0.513-0.733)	0.148	0.711
Sum variance	0.604	(0.493-0.715)	0.317	0.868
Sum entropy	0.649	(0.538-0.760)	0.0186	0.123
Inf mea of corr1	0.719	(0.609-0.829)	0.000140	0.000770
Inf mea of corr2	0.498	(0.378-0.618)	0.944	0.506
F1	0.605	(0.500-0.710)	0.149	0.128
BP excl tumor more than 10%	0.557	(0.445-0.670)	0.381	0.317
BP excl tumor (10-100%)	0.564	(0.452-0.676)	0.438	0.420
(variance/mean) BP excl tumor (10-100%)	0.557	(0.446-0.668)	0.402	0.446

AUC = area under the curve, NA = data not available. The adjusted *P*-value was determined by correcting for multiple hypothesis testing. The feature “major axis” was used as the control. The first block of features describe tumor morphology, the second block describes tumor texture, and the third block describes MRI enhancement.